What is the significance of pore pressure in a saturated shale layer?

J. Goncalves, Pauline Rousseau-Gueutin, G. de Marsily, P. Cosenza, S. Violette

What is the significance of pore pressure in a saturated shale layer?

J. Gonçalvès,[1,2] P. Rousseau-Gueutin,[1,3] G. de Marsily,[1,4] P. Cosenza,[1,5] and S. Violette[1,4]

Received 7 April 2009; revised 22 September 2009; accepted 23 October 2009; published 29 April 2010.

[1] Electrostatic interactions, associated with negatively charged surfaces of clay minerals, produce a so-called "disjoining pressure" when diffuse layers overlap, i.e., at low porosity. Disjoining pressure is the pressure difference between the water in the clay pore space and that in a bulk solution at the same depth. Another widely used concept in clay-rocks is the "swelling pressure." It corresponds in fact to the macroscopic average of the disjoining pressure. This study proposes to determine the value of the swelling pressure of a natural material by a simple volume-averaging approach of the disjoining pressure, calculated for each clay mineral present in the material. The swelling pressure, which is dependent on the salinity of the pore fluid, is introduced into a hydrochemomechanical coupling, yielding a more general pressure diffusion equation. The results are compared to swelling pressure measurements for natural shale samples. The implications of this swelling pressure for water pressure measurements in natural formations are also discussed.

Citation: Gonçalvès, J., P. Rousseau-Gueutin, G. de Marsily, P. Cosenza, and S. Violette (2010), What is the significance of pore pressure in a saturated shale layer?, *Water Resour. Res.*, *46*, W04514, doi:10.1029/2009WR008090.

1. Introduction

[2] Pore pressure in a clay material is challenging to measure due to the low filtration rates in such media. Estimating the pressure field in the porosity of a shale layer is nevertheless crucial to identify the Darcy velocity through this medium. Furthermore, in case of a substantial Peclet number, this velocity comes into play for solute transport in the so-called advective term of the dispersion-advection equation [*de Marsily*, 1986; *de Marsily et al.*, 2002]. The great difficulty of acquiring pressure fields as well as the small fluxes, explain the low interest so far in such measurements. Pressures are usually measured in the surrounding aquifers in order to estimate leakage fluxes. However, some in situ pressure measurements in shales are currently made in the context of research on the feasibility of nuclear waste repositories in deep geological formations. This in situ pressure is denoted as hydrostatic or bulk pressure hereafter. The specificity of the clay mineral structure, associated with its surface charge, has prompted scientists to consider specific forces that can affect the pressure in the pores of such materials. In that respect, besides the hydrostatic pressure, two major concepts predominate in the abundant literature devoted to clay-rocks (see reviews by *Mitchell* [1993] and *Horseman et al.* [1996]): the disjoining pressure and the swelling pressure. Consequently, in clay-rich materials, three pressures; that is, hydrostatic, disjoining and swelling pressure have to be considered. *Bennethum and Weinstein* [2004] discussed this diversity in terms of bulk, thermodynamic and swelling pressures. In the present paper, we analyze and discuss their real hydrodynamic significance as well as the relations between these three pressures.

[3] At the sample scale, the hydrostatic pressure is the pressure that can be measured (or prescribed) in reservoirs in contact with the clay-rock sample. In geological formations, hydrostatic pressures are measured in closed chambers, e.g., limited by two packers in a borehole. Introduced in colloidal sciences at the beginning of the 20th century [*Langmuir*, 1938; see also *Derjaguin et al.*, 1987], the disjoining pressure is defined as the pressure difference between a thin film of fluid present between two platelets of a clay mineral and the solution (termed bulk or equilibrium solution) where these possibly charged platelets are embedded. This pressure difference which only exists when interfacial zones (e.g., the diffuse layer) overlap is attributed to surface forces (e.g., of electrostatic nature) that differ from the simple gravity in the bulk solution. This concept can be applied to clay-rock systems where the pore water is located between charged clay particles. The disjoining pressure is thus a microscopic concept which must be analyzed at the pore scale. The macroscopic swelling pressure which can be measured in natural materials [see, e.g., *Madsen and Vonmoos*, 1985; *Huang et al.*, 1986; *Wong*, 1998] is associated with the well-known swelling properties of certain clays (e.g., smectite). This pressure is currently described as the external stress that has to be applied to a clay-rock sample in order to maintain its mechanical equilibrium (prevent swelling). This external stress is then equated to the pore pressure. By this

[1]Sisyphe, UMR 7619, Université Pierre et Marie Curie, Paris, France.
[2]CEREGE, UMR 6635, CNRS, Aix en Provence, France.
[3]Now at School of the Environment, Flinders University, Adelaide, South Australia, Australia.
[4]Sisyphe, UMR 7619, Université Pierre et Marie Curie, CNRS, Paris, France.
[5]Now at HydrASA, FRE 3114, ESIP, Université de Poitiers, CNRS, Poitiers, France.

0043-1397/10/2009WR008090

experimental definition, the swelling pressure is a macroscopic concept which applies to a representative elementary volume (REV, e.g., a sample).

[4] In this paper, the question that we discuss is the possible occurrence of a disjoining pressure in the porosity of a compacted clay-rock and its potential impact. How can we describe and introduce such a pressure in the hydrogeological formulation of groundwater flow and solute transport? Are pressure gages embedded in shale layers influenced by this local disjoining pressure? In order to answer all or part of these questions, it is necessary to return to the theory of pressure structure in thin films introduced by interface physicists. In their theoretical analysis of surface forces, *Derjaguin et al.* [1987, p. 282] conclude that the swelling pressure represents in fact the macroscopic average disjoining pressure. Since it is associated with a deformation of a clay-rich porous medium, the swelling pressure should be considered in the hydromechanical coupling accounted for in transient hydrodynamic calculations. Certain authors introduced explicitly the notion of disjoining pressure or surface forces in their hydrochemomechanical models [see, e.g., *Barbour and Fredlund*, 1989; *Hueckel*, 1992; *Bennethum et al.*, 1997; *Murad and Cushman*, 1997, 2000], in the framework of poroelasticity. Other ones followed directly a thermomechanical development for deforming porous media [*Coussy*, 2004] in the framework either of elastoplasticity (e.g., the cam-clay approach [*Loret et al.*, 2002] or elasticity [*Heidug and Wong*, 1996]) without introducing explicitly microscopic surface force concepts. Despite their rigor, the practical use of these latter approaches for hydrogeological applications is difficult, computer time consuming and their parameter determination is often problematic. The extension to electrochemical interactions of "Terzaghi's type" hydromechanical coupling introducing explicitly the notion of disjoining pressure offers a more convenient (although simplified) and practical approach. This is the approach which is followed in this paper. For those studies which accounted for the surface forces explicitly, alternative conceptual basis with respect to the disjoining pressure were considered. Some authors considered a disjoining pressure almost equivalent to its electrostatic ("osmotic") component [*Barbour and Fredlund*, 1989; *Hueckel*, 1992; *Moyne and Murad*, 2002; *Revil et al.*, 2005] while others considered the "hydration" or structural forces as prominent [*Bennethum et al.*, 1997; *Murad and Cushman*, 1997, 2000] following the view advocated by *Low* [1987]. Here, no a priori assumption on the relative importance of the different components of the disjoining pressure is made. In addition, in the previous studies, the way to obtain disjoining pressure and then swelling pressure relationships as a function of the salinity of the equilibrium solution and the mean interparticle spacing is often left to the reader's appreciation (except for the partial data of *Low* [1987]). In the present work, a synthetic view of the available microscopic disjoining pressure data for expansive clays which allows identifying such relations is proposed. The swelling pressure is then introduced in the hydromechanical coupling proposed, e.g., by *de Marsily* [1986] to establish a simple and practical pressure diffusion equation involving an explicit electrochemical term. The corresponding equation is then compared to experimental results.

[5] In the first part, after a brief outline of the electrochemical properties of clays, the concept of disjoining pressure is presented and reviewed. Then, some disjoining pressure data for 2:1 swelling clay minerals are used in a simple averaging approach to estimate the macroscopic swelling pressure for natural materials. Finally, the hydrodynamic consequences of the swelling pressure are analyzed especially by the introduction of a simple electrochemical storage term in the pressure diffusion equation used in hydrogeology.

2. Pore Pressure in Clay Materials: Theoretical Background

2.1. Electrical Properties of Clay-Rocks

[6] Due to isomorphic substitutions in the crystal lattice as well as to complexation reactions at the surface of the minerals, these lattices are characterized by a negative surface charge at natural pH values [see, e.g., *Mitchell*, 1993; *Horseman et al.*, 1996; *Sposito et al.*, 1999]. An electric field related to an electrical potential distribution develops in the pore space between clay surfaces. This electrical potential decreases (in absolute value) from the surface toward zero within an equilibrium solution or toward the midplane if this equilibrium solution is not reached. Ions of opposite charge are attracted by electrostatic forces. These ions, referred to as counterions, balance the negative charges guaranteeing the overall electroneutrality of the medium. The counterions are distributed between a compact layer (Stern layer) and a more dispersed layer (diffuse layer). These interactions are represented schematically in Figure 1 in the case of truncated adjacent diffuse layers. The equilibrium solution is an important concept in interface sciences. It is the solution that would be at total thermodynamic equilibrium with the solution present in the porosity of the shale. In an infinitely developed diffuse layer, it is the solution at some distance from the surface where the electrical influence vanishes. As described below, it can also be seen as the bulk solution of a reservoir in contact and at local equilibrium with a clay material. But, according to *Coussy* [2004], this solution is generally fictitious within a real shale layer (as illustrated in Figure 1). In the following, a subscript 'f' is used to denote the properties and variables in the equilibrium solution. The distribution of the counterions can be calculated from Boltzmann's distribution [see, e.g., *Van Olphen*, 1963; *Mitchell*, 1993]:

$$c^i = c_f^i \exp\left(-\frac{q_i \varphi}{k_B T}\right), \tag{1}$$

where c^i (ions m^{-3}) is the concentration of ion i in the pore space, c_f^i is its concentration in the equilibrium solution (see below), q_i (C) is the ionic charge ($\pm\nu_i e$ where ν_i is the valence, $e = 1.6\ 10^{-19}$ C is the elementary charge), k_B is the Boltzmann constant (1.3810^{-23} J K^{-1}), φ is the electrical potential (V) and T the temperature (K) (see the notation section).

[7] Different models accounting for these interactions between pore fluid electrolytes and charged surfaces are available. They allow the calculation of the electrical potential distribution as a function of the distance to the charged surfaces. Among these models, electrical triple

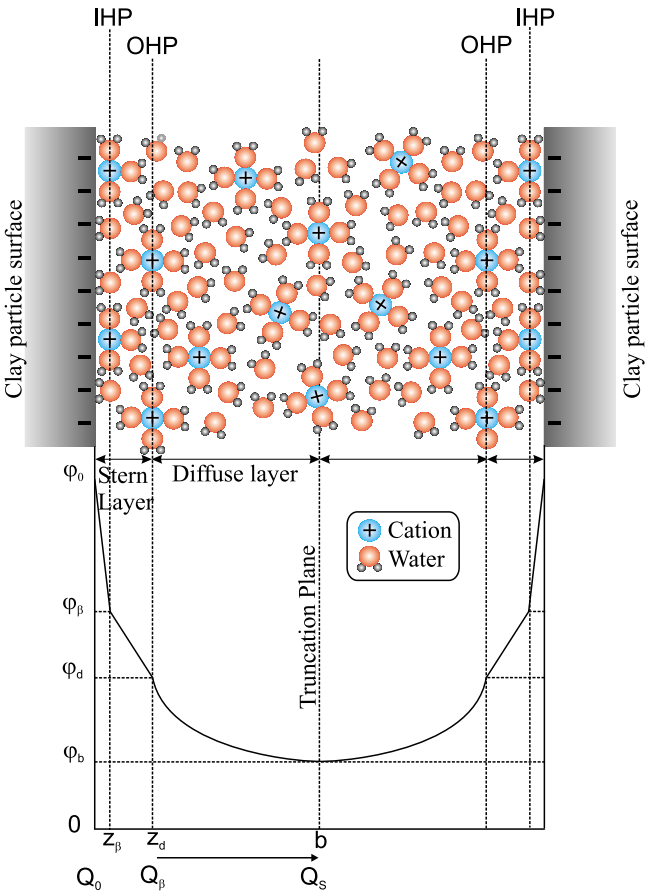

Figure 1. Schematic representation of the ion surface interaction in the case of a truncated diffuse layer with the electrochemical variables of the triple layer model (TLM). All the electrical potentials φ_i are in V, and the surface charges Q_i are in C m^{-2}. Q_0, Q_β, and Q_S are the charge density at the surface, in the Stern layer, and in the diffuse layer. IHP and OHP stand for inner and outer Helmoltz plane, respectively.

layer models (TLM) describe the distribution of the ions within the porosity using three domains [see, e.g., *Davis and Leckie*, 1978; *Hiemstra and Van Riemsdijk*, 1996; *Leroy and Revil*, 2004; *Gonçalvès et al.*, 2007]: (1) the Stern layer is a compact layer formed by ions that are directly bound to the surface (covalent or ionic bonds) plus strongly attracted hydrated ions [*Sposito et al.*, 1999]; (2) the diffuse layer, where the ions are attracted by the surface but more dispersed, which is thus considered as part of the solution; and (3) the last layer, when it exists, which is the free electrolyte or equilibrium solution where the electrical field is null and where the electroneutrality is achieved by the ionic balance. These models, introducing a compact Stern layer, are known as Stern-Grahamme models. If the Stern layer is absent (a diffuse layer directly in contact with the surface), the models are referred to as Gouy-Chapman models. The latter overestimate the ionic concentrations as ions are considered as point charges while the Stern-Grahamme models take into account the finite size of ions [*Mitchell*, 1993; *Horseman et al.*, 1996]. In a TLM, surface reactions such as complexation or protonation/deprotonation are taken into account at the solid surface and in the Stern layer. These reactions make it possible to calculate and no longer to impose the surface charge densities and the electrical potentials close to the mineral surface. In the diffuse layer, the description of the electrical potential distribution is obtained through the resolution of the Poisson-Boltzmann equation, which for a single cation and anion of the same valence ν_f, and assuming the ideality of the solution [see, e.g., *Van Olphen*, 1963; *Mitchell*, 1993] is

$$\frac{d^2\varphi}{dz^2} = \frac{2c_f\nu_f e}{\epsilon}\sinh\left(\frac{\nu_f e\varphi}{k_B T}\right), \tag{2}$$

where ϵ (F m^{-1}) is the permittivity of the solution, $c_f = c_f^- = c_f^+$, c_f^- and c_f^+ are the concentration of the anion and the cation in the equilibrium solution (ions m^{-3}) and z is the axis perpendicular to the solid surface. Once the electrical potential distribution is known, the concentration can be calculated from equation (1). Figure 1 summarizes this brief description in the case of a Stern-Grahamme model and presents the main variables to be estimated with a TLM. A classical parameter in the domain of interface science is the Debye length $1/\kappa$ which provides an order of magnitude of the diffuse layer thickness:

$$\frac{1}{\kappa} = \sqrt{\frac{\epsilon k_B T}{2c_f e^2 \nu_f^2}}. \tag{3}$$

Typical values for the Debye length are discussed by *Horseman et al.* [1996] for monovalent ions such as Na^+, Cl^-. This length is almost 10 nm at $c_f = 10^{-3}$ mol L^{-1} and 3 nm at $c_f = 10^{-2}$ mol L^{-1}. If the lengths are compared to classical values of the pore size in a compacted clay, i.e., from a few nanometers to a few tens of nanometers, it can be seen that the diffuse layers of adjacent charged surfaces are probably interacting [*Mitchell*, 1993] creating a truncated diffuse layer as shown in Figure 1. The pore space as described in Figure 1 represents approximately the porous medium structure as it is generally considered by hydrogeologists, the Stern layer corresponds to the adsorbed layer of fluid accounted for in the concept of kinematic porosity [see, e.g., *de Marsily*, 1986]. From Figure 1, it can also be seen that the pore space corresponding to the diffuse layer is subjected to an electric field. In case of overlap, the overall interplatelet space is subjected to this electric field which is perpendicular to the clay mineral surfaces. This electric field and related ionic content is thought to strongly modify water properties such as density or viscosity in the first nanometer from the surface [see, e.g., *Martin*, 1960; *Mitchell*, 1993; *Hribar et al.*, 2002; *Gonçalvès and Rousseau-Gueutin*, 2008]. As described in the introduction, it is plausible that the pore fluid pressure is influenced by, e.g., the electrostatic forces specifically at work in such media (aquitards), whereas they are absent in more classical hydrogeological formations (sands, limestone).

2.2. Surface Forces and Disjoining Pressure

[8] At the end of the 1930s, interface scientists working on colloids showed that the pressure in water films between two charged particles differs from the pressure of water at the same depth in the reservoir containing these particles [*Langmuir*, 1938; *Derjaguin*, 1939] (cited by *Derjaguin et al.*, 1987]). They attributed this difference to electrostatic

and molecular interactions between the charged surfaces and the interplate electrolyte. The more extensive and quantitative development proposed by *Derjaguin et al.* [1987] is reviewed below. Note that in a more intuitive and qualitative approach, *Langmuir* [1938] obtained similar results. A full discussion on the conceptual differences between the two approaches can be found in work by *McBride* [1997]. According to *Derjaguin et al.* [1987, p. 27], this "departure from the hydrostatic law" only occurs if the interfacial zones, here the diffuse layers, overlap. If there is no overlap (large pore size or high-concentration solutions), the intensive variables such as pressure are equivalent to those in the bulk or equilibrium solution. This difference in pressure, named disjoining pressure, is caused by the action of surface forces induced by the overlap. Two types of surface forces can be identified: repulsive and attractive. Repulsive and attractive forces per unit surface area are translated into positive or negative (traction in a mechanical sense) pressure, respectively. The balance between these two kinds of forces per unit surface area determines the sign of the disjoining pressure. Furthermore, noting that the surface forces at work in overlap conditions are mostly perpendicular to the surface (in the direction of the electric field), these authors argue that the "pressure" in thin films is no longer a scalar but becomes a tensor. This result was established by *Derjaguin et al.* [1987] by writing a generalized Maxwell stress tensor, i.e., the stress tensor for a body under the influence of an electromagnetic field. This consists in encapsulating the hydrostatic pressure, electrostatic and molecular forces per unit surface in a generalized "pressure" whose anisotropy is imposed by the surface forces. Hence, this fluid "pressure" in a film adjacent to clay surfaces is no longer a pressure in the strict sense but has the significance of a local stress, which, in the local coordinate system attached to the clay surfaces, is

$$\mathbf{p}_{oxyz} = \begin{vmatrix} p_{xx} & 0 & 0 \\ 0 & p_{yy} & 0 \\ 0 & 0 & p_{zz} \end{vmatrix}, \tag{4}$$

where the z axis is perpendicular to the clay surface. Refining their initial definition, *Derjaguin et al.* [1987] interpreted the disjoining pressure as the difference between the pressure normal to the solid surfaces in the film, i.e., the direction of surface forces, and the pressure in the equilibrium solution. This concept, that introduces an alteration of the "pressure structure" (anisotropy and contrast in pressure), is illustrated below by writing a local volume force balance to identify one of the components of the disjoining pressure. In fact, these authors identify two main components of the disjoining pressure, a repulsive electrostatic component and an attractive molecular or Van der Waals component. The extensively used electrostatic component of the disjoining pressure can be formally established by a thermodynamic or a mechanical approach. According to *Derjaguin et al.* [1987], the mechanical volumetric force balance equation within a film of water between two charged surfaces imbedded in a bulk (equilibrium) solution is

$$grad(p) + \rho grad(\varphi) + grad\left(\frac{1}{2}\frac{d\epsilon}{d\rho_f}\rho_f E^2\right) = 0, \tag{5}$$

with $p(z, b)$ (Pa), the hydrostatic pressure, ρ the charge density (C m^{-3}) in the film of solution [see *Van Olphen*, 1963], φ (V) is the electrical potential, ρ_f the density of the fluid (kg m^{-3}), ϵ (F m^{-1}) is the permittivity of the fluid and E the electric field (V m^{-1}). The second term on the left-hand side of equation (5) is the electric force acting on the volume charge and the third term is the so-called electrostriction term (force due to orientation of water molecules subjected to an external electric field [see *Stratton*, 1941]). An algebraic treatment, which is detailed in Appendix A, allows us to obtain the following expressions for the components $p_{xx} = p_{yy} = p_T$ and $p_{zz} = p_N$ where p_N and p_T are the components of "pressure" **p** normal and tangential to the surface, respectively:

$$p_N = p_f + \pi_D^e \tag{6}$$

$$p_T = p_f + \frac{1}{\epsilon}\frac{d\epsilon}{d\rho_f}\rho_f \pi_D^e + \left(\frac{1}{\epsilon}\frac{d\epsilon}{d\rho_f}\rho_f - 1\right)\int_0^{\varphi} \rho d\varphi, \tag{7}$$

where φ is the electrical potential at a distance z from the surface (virtually $\varphi = 0$ at an infinite distance) and with

$$\pi_D^e = -\int_0^{\varphi_b} \rho d\varphi, \tag{8}$$

where π_D^e (Pa) is the electrostatic component of the disjoining pressure, φ_b (V) is the electrical potential at the midplane (see Figure 1) and p_f is the hydrostatic pressure in the equilibrium solution. This component is independent of z and depends only on the distance between clay platelets. In the case of adjacent surfaces of equivalent charge and for a monovalent and symmetric salt (e.g.,NaCl), it is

$$\begin{aligned} \pi_D^e &= 2k_B T c_f \left(\cosh\left(\frac{e\varphi_b}{k_B T}\right) - 1\right) \\ &= k_B T\left(c^+ + c^- - 2c_f\right)_{z=b}, \end{aligned} \tag{9}$$

where c^+ et c^- (ions m^{-3}) are the concentrations of the cation and the anion in the porosity and c_f is the concentration of these ions in the equilibrium solution. Unlike the normal component, the transverse one is dependent of the distance to the surface. This illustrates the tensorial property of the total "pressure" introduced by *Derjaguin et al.* [1987]. It should be noted that an alternative way to identify the electrostatic component of the disjoining pressure π_D^e is to use mean concentrations calculated from Donnan equilibrium [*Jougnot et al.*, 2009]. This view is a direct continuation of the pioneering work of *Langmuir* [1938].

[9] Besides the electrostatic component of the disjoining pressure, others are also considered in the literature. *Derjaguin et al.* [1987] introduce a second component which is an attractive Van der Waals term corresponding to a weak attraction between the molecules of the adjacent surfaces. It can be accounted for by using the relationship

$$\pi_D^{vdw} = -\frac{A}{6\pi(2b)^3}, \tag{10}$$

where A is the Hamaker constant dependent on the mineralogic nature of the surface and $2b$ is the distance between the two particles. For mica and water films, a value of A of

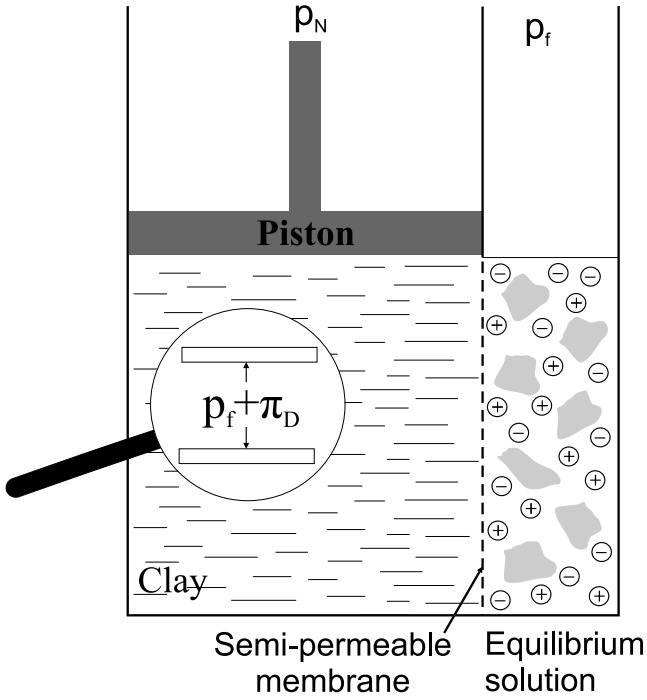

Figure 2. Schematic representation of the measurement method of the disjoining pressure according to *Low* [1987].

2 10^{-20} J has been reported [*Derjaguin et al.*, 1987]. These two repulsive and attractive components are used in the so-called DLVO (Derjaguin-Landau-Verview-Overbek) theory of the stability of colloidal suspensions which considers the following expression:

$$\pi_D = \pi_D^e + \pi_D^{vdw}. \tag{11}$$

These concepts, formally developed by *Derjaguin et al.* [1987] (see also historical discussion by *Churaev* [2003]), are supported by numerous experimental studies (see section 3.2 where we review some of them). According to *Derjaguin et al.* [1987], this disjoining pressure, which is thus a consequence of a local stress balance, can be measured by applying an external pressure to maintain the interplatelet in mechanical equilibrium. In fact, this describes exactly the process of a swelling pressure measurement depicted in Figure 2. They consider that the swelling pressure is, at the macroscale, the volume average of the disjoining pressure. However, another component is discussed and debated in the literature [*Viani et al.*, 1983; *Derjaguin et al.*, 1987; *Horseman et al.*, 1996; *McBride*, 1997]. Indeed, the DLVO theory cannot explain certain experimental data as claimed by, e.g., *McBride* [1997] and also previously recognized by *Derjaguin et al.* [1987]. An additional term besides the electrostatic and molecular components has been proposed. This term is related to the solid surface hydration with the presence of several monolayers of water molecules with a modified structure of the hydrogen bond network as compared to the equilibrium solution. This has long been reported in the literature through the observation of the alteration of water properties such as density or viscosity in the first nanometer from the surface [see, e.g., *Martin*, 1960; *Mitchell*, 1993]. When the interplatelet distance is small, these monolayers of structurally specific water overlap, and an additional repulsive term, the so-called structural component of the disjoining pressure π_D^s, has to be introduced [*Derjaguin et al.*, 1987]. To our knowledge, the only theoretical development concerning this hydration force component has been proposed by *Marcelja and Radic* [1976]. The theory is however semiempirical; that is, the parameters in the theoretical expression of this component must be fitted on data. According to these authors, the hydration component can be described by the exponential relation

$$\pi_D^s = \kappa \exp\left(-\frac{2b}{\lambda}\right), \tag{12}$$

where κ and λ are coefficients that have to be experimentally determined. For quartz and mica, values in the range 7 10^5 to 10^7 Pa for κ and 0.8 to 1 nm for λ are reported [*Derjaguin et al.*, 1987]. In the absence of a fully predictive theory, this component is always determined empirically by the difference between the measurement of the disjoining pressure and the DLVO theory. It is considered as the main component for interparticle distances between 1.5 and almost 5 nm [*Israelachvili and Pashley*, 1983; *McGuiggan and Pashley*, 1988]. According to *Low* [1987], this component could even be the main component of the swelling pressure whatever the pore size.

[10] Once recognized, these components are assumed to be linearly additive, which is consistent with a force balance analysis. Expressions such as

$$\pi_D = \pi_D^e + \pi_D^{vdw} + \pi_D^s \tag{13}$$

can be found. The previous expressions for components p_N and p_T, i.e., equations (6) and (7), were obtained by considering only the electrostatic surface forces. As suggested by *Derjaguin et al.* [1987, chapter 2], the molecular and hydration forces should be introduced in the expressions of p_N and p_T yielding

$$p_N = p_f + \pi_D^e + \pi_D^{vdw} + \pi_D^s \tag{14}$$

$$p_T = p_f + \frac{1}{\epsilon}\frac{d\epsilon}{d\rho_f}\rho_f \pi_D^e + \left(1 - \frac{1}{\epsilon}\frac{d\epsilon}{d\rho_f}\rho_f\right)\int_0^{\varphi} \rho d\varphi + \pi_D^{vdw} + \pi_D^s. \tag{15}$$

In the following, the applicability of these concepts to clay-rock systems and their modeling are analyzed. The disjoining pressure being a microscopic concept, a first stage of upscaling to identify the macroscopic swelling pressure is required.

3. Estimating the Macroscopic Swelling Pressure of Clay-Rocks

3.1. Relationship Between Disjoining and Swelling Pressures

[11] The initial work by *Langmuir* [1938] and *Derjaguin et al.* [1987] predicts a higher pressure in the porosity of a shale than in adjacent uncharged media provided that the diffuse layers of the clay platelets overlap. These concepts have been developed primarily at the microscopic scale for colloidal suspensions to describe the stability of particles that can coagulate or disperse when no external stress is

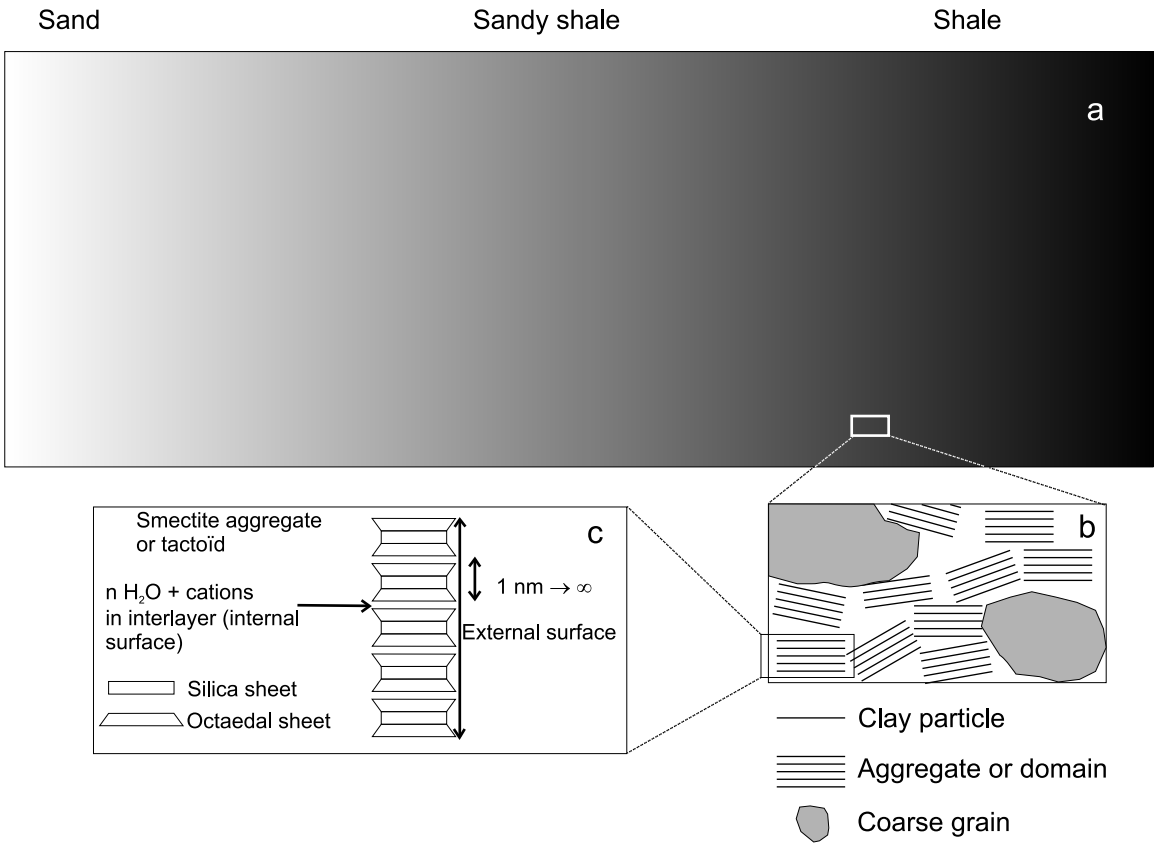

Figure 3. (a) Schematic view of the heterogeneity of a natural clay-rock. (b) Petrofabric showing the coarse grains and the clay particles organized as stack or aggregates. (c) A smectite tactoid showing the internal surfaces (involved in swelling) and the external surfaces.

applied. But these concepts can also apply to compacted clay-rocks characterized by a low porosity. Indeed, such pressures can exist only in case of a developed microporosity associated with short interplatelet distances that enable the diffuse layers to overlap. In clay-rocks, if clay particles have been clustered together by compaction, they are maintained in this compacted state by the all-around confining stress and the rigidity of the rock. Despite the rigidity and the existence of a confining pressure, clay-rocks are currently characterized by their swelling properties and authors invoke the so-called swelling pressure. What might be the link between the swelling pressure and the disjoining pressure? The "osmotic" swelling pressure was formally defined by, e.g., *Coussy* [2004] in exactly the same manner as *Derjaguin et al.* [1987] and *Langmuir* [1938] use to express the electrostatic component of the disjoining pressure in equation (9). Furthermore, *Derjaguin et al.* [1987] describe the swelling pressure as an estimate of the average disjoining pressure over the clay-rock volume. Consequently, from a theoretical standpoint, the swelling pressure for a macroscopic volume of a natural clay-rock can be obtained by a volume averaging of the microscopic disjoining pressure.

[12] The swelling pressure of a clay is classically measured at the sample scale. It is estimated as the confining stress exerted by a triaxial apparatus to maintain constant the volume of the sample, or the stress exerted by a piston at the sample equilibrium. This swelling occurs for instance when a core sample is exposed to a solution of lower salinity than the natural formation solution. This swelling behavior is associated with the presence of 2:1 clay minerals, i.e., smectite or illite with a prominent role of the former due to its high specific surface (750 $m^2\ g^{-1}$) [*Mitchell*, 1993]. Indeed, when smectite minerals swell, water is attracted between the internal surfaces (interlayers, see Figure 3c) which characterize exclusively this mineral. According to *Mitchell* [1993], two concepts to describe the swelling are used, the "osmotic" pressure and the surface hydration effects. The former is associated with the electrostatic repulsive force which is accounted for in the electrostatic component of the disjoining pressure. The second one corresponds to an alteration of the chemical potential of water due to surface interactions yielding a converging flow toward the internal surfaces of smectite minerals. A self-consistent approach is obtained by introducing the surface hydration effects into a general expression of the disjoining pressure (see equation (13)). In order to perform a simple volume averaging of the microscopic disjoining pressure, reference data for the swelling minerals should be considered.

3.2. Experimental Identification of the Disjoining Pressure for 2:1 Clay Minerals

[13] Three experimental protocols have been used to measure the disjoining pressure of pure clay minerals as a function of particle spacing and electrolyte concentration. The first experimental apparatus is a compressional cell corresponding to the schematic representation in Figure 2.

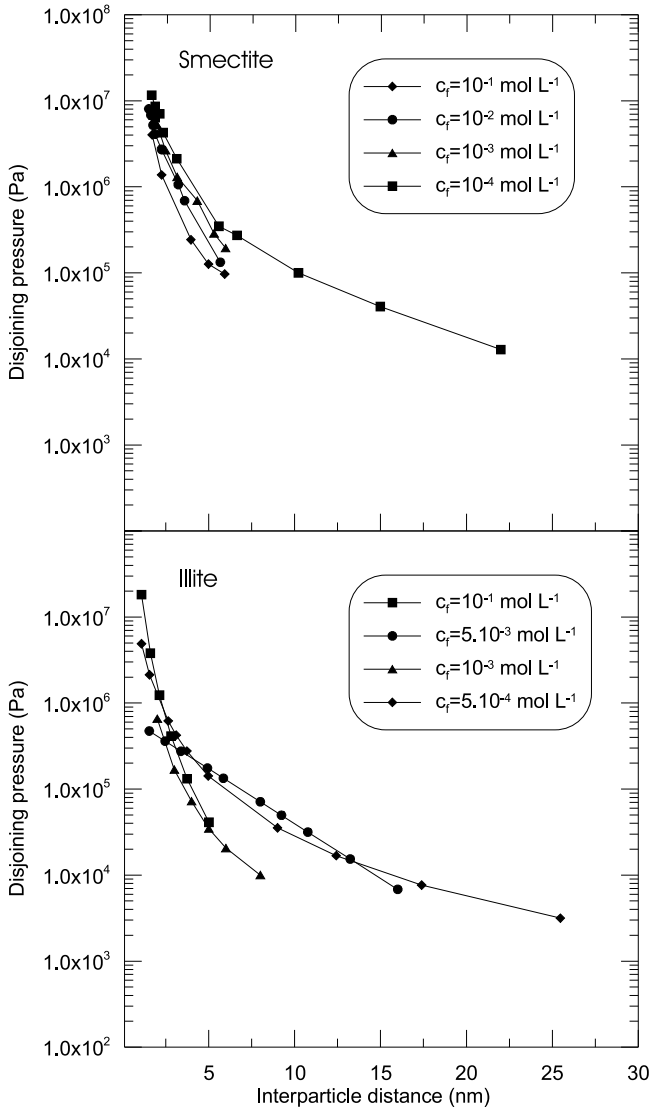

Figure 4. Disjoining pressure data as a function of the interparticle distance and the salinity. Data for illite (mica) are from *McGuiggan and Pashley* [1988], *Pashley* [1981], and *Quirck* [1986]; data for smectite are from *Barclay and Ottewill* [1970] and *Callaghan and Ottewill* [1974].

Such mechanical measurements were performed by, e.g., *Barclay and Ottewill* [1970], *Callaghan and Ottewill* [1974], or *Viani et al.* [1983] using oriented montmorillonite gels so that the clay particle bedding is perpendicular to the piston, thus measured pressures (stresses) are perpendicular to the clay surfaces. During the experiments of *Viani et al.* [1983] for instance, the samples were placed in a chamber between a piston and a ceramic plate in contact with a NaCl solution at a salinity of 10^{-4} mol L^{-1} and at atmospheric pressure. Increasing pressure steps were applied by the piston causing a reduction in interplate separation. After equilibration for each step, the swelling pressure is equal to the pressure applied by the piston and the clay interplate spacing was measured by X-ray diffraction. Disjoining pressures as high as several bars were thus measured in the direction perpendicular to the surfaces when the pressure in the adjacent reservoir was 1 bar. The more extensive results obtained by *Callaghan and Ottewill* [1974] for Na-Montmorillonite (smectite) are shown in Figure 4. Figure 4 shows a clear decrease of the disjoining pressure as the interparticle distance or the concentration increases. In such experiments, the interparticle spacing between the clay platelets of the macroscopic sample is believed to be homogeneous. Consequently, the macroscopic swelling pressure equals the microscopic disjoining pressure while it is more generally a volume average of the disjoining pressure (see section 3.1).

[14] The second experimental method is the surface force apparatus which was developed in the 1970s and subsequently modified to allow surface force measurements for materials immersed in electrolyte solutions [*Israelachvili and Adams*, 1978; *Israelachvili and Pashley*, 1983]. In these experiments, two orthogonally positioned cylindrical surfaces of radius R (≈1 cm) covered with clay sheets are brought into close contact step by step. At each step, the interaction force F and the distance between the two crossed cylinders B are measured. For practical use in clay materials characterized by a platy shape, it is desirable to estimate the equivalent force per solid unit surface that would have been measured between two plane-parallel surfaces separated by the same distance B ($2b$), i.e., the disjoining pressure π_D. For this purpose, the following approximation by *Derjaguin et al.* [1987, p. 46] can be used:

$$\frac{F}{R} = 2\pi \int_B^\infty \pi_D(B) dB. \tag{16}$$

Noting that the relation between the disjoining pressure and the interparticle distance corresponds to a power law or an exponential decay, the derivative of equation (16) relative to B is defined and yields

$$\pi_D(B) = \frac{1}{2\pi} \frac{d\left(\frac{F}{R}\right)}{dB}. \tag{17}$$

The surface force apparatus was widely used in the 1980s and 1990s for mica surfaces by *Pashley* [1981], *McGuiggan and Pashley* [1988], and *Quirk and Pashley* [1991]. Some interpreted measurements (using equation (17)) for Na-mica (equivalent to Illite [*Quirk*, 1986]) are depicted in Figure 5. Although less obvious, similar trends as for smectites are obtained. The disjoining pressure is generally lower for illite than for smectite (up to 1 order of magnitude).

[15] The last experimental method to measure surface forces at the microscopic scale uses the atomic force microscope [see, e.g., *Li et al.*, 2007]. The force between two microscopic spherical samples (few micrometers) placed at a certain distance are measured. This distance is varied during the experiment. For two identical spherical particles of radius R, another approximation for the equivalent plane-parallel force per unit surface at the same distance is available and writes [*Derjaguin et al.*, 1987, p. 46]

$$\frac{F}{R} = \pi \int_B^\infty \pi_D(B) dB. \tag{18}$$

Upon derivation, this equation provides a useful expression for the disjoining pressure in plane-parallel geometry.

[16] The first method provides a direct estimate of the disjoining pressure while the two others require an intermediate algebraic treatment. Therefore, besides the theo-

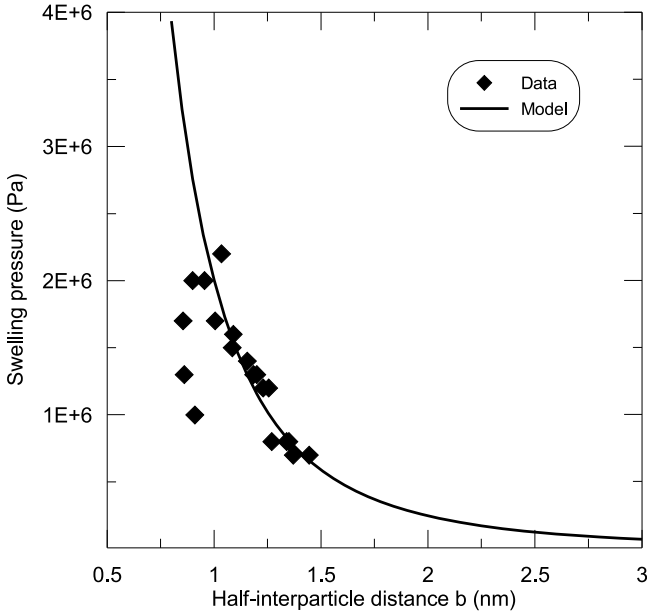

Figure 5. Swelling pressure measured for the Opalinus clay by *Madsen and Vonmoos* [1985]. The model is the simple volume-averaging approach of equations (20) and (21).

retical expressions discussed in section 2.2, the experimental protocols described above offer an alternative identification of the disjoining pressure, possibly combined with expressions (16) or (18). Whatever the technical choice for measuring the interaction between clay particles, such experiments support the view of *Derjaguin et al.* [1987] of an anisotropic "pressure" in water films with different directional components. Although the experimental materials are clay gels or isolated particles and not clay-rocks, these experiments give valuable data since both pore size and disjoining pressures are provided. Note that only the total disjoining pressure for pure materials but not the different components of this pressure is measured in such experiments. The different components should be estimated by means of theoretical expressions and models. The electrostatic component can be calculated from equation (9) where the concentrations are determined using an electrical model. This was done for bentonite in previous work [*Gonçalvès et al.*, 2007]. For practical use on natural materials, the attractive molecular component can be neglected since it becomes significant only for interparticle distances lower than 0.5 nm. The identification of the third component, the structural disjoining pressure, is more difficult. Since no fully predictive theory has been proposed so far, only experimental work can be used to identify this component as a function of the interparticle distance and the concentration. In this paper, the total disjoining pressure containing all the components is considered but we do not go into more detail concerning this component.

3.3. Simple Averaging Approach to Estimate the Swelling Pressure of Natural Clay-Rocks

[17] Our goal in this section is to derive a useful expression for the macroscopic swelling pressure from the microscopic expressions of the disjoining pressure. A natural clay-rock is characterized by an ensemble of pure clay minerals and coarse grains (e.g., quartz, calcite [see *Marion et al.*, 1992]) which are usually described using volumetric fractions. A schematic view of this heterogeneity is shown in Figure 3a with a representation of the petrofabric involving aggregates in Figure 3b. In order to obtain an expression of the swelling pressure for macroscopic clay samples, some volume averaging of the microscopic disjoining pressure for pure clay end-members must be done. Since the disjoining pressure is associated with surface interactions, this volume averaging should involve the surface fractions exposed to the pore fluid for each type of clay minerals. Here, we propose to carry out the volume averaging by estimating the surface fraction of each end-member (e.g., smectite, illite, kaolinite) in a unit volume of porous medium. Neglecting the contribution of the coarse grains to the overall surface due to their low specific surface compared to the clay minerals, this surface fraction writes

$$f_S^i = \frac{A_S^i f_{wt}^i}{\sum_k A_S^k f_{wt}^k}, \tag{19}$$

where f_S^i, f_{wt}^i and A_S^i are the nondimensional surface and weight fractions and the specific surface ($m^2\ g^{-1}$) of clay mineral i, respectively. Then, this quantity can be used as a weight for the disjoining pressure characterizing each mineral to estimate the macroscopic swelling pressure $\langle \pi_D \rangle$ such as

$$\langle \pi_D \rangle = \sum_k f_S^k \pi_D^k. \tag{20}$$

It must be stressed here that this approach requires the transposition at the macroscopic scale of two crucial variables which determine the value of the microscopic disjoining pressure, i.e., the equilibrium concentration c_f and the interparticle spacing. Unlike the experiments described in section 3.2, these two quantities are obtained with low precision in natural materials. The equilibrium concentration can be obtained by squeezing experiments or by modeling the geochemical equilibrium between the minerals and the pore fluid. The mean pore size ($2b$) can be identified by the following simple mass balance equation assuming a parallel plane geometry [*Neuzil*, 2000]:

$$\omega = (1 - \omega)\rho_S A_S b, \tag{21}$$

where ω is the total porosity, ρ_S is the density ($kg\ m^{-3}$) of the solid and A_S is the total or external specific surface (see below).

[18] This simple analysis was applied to a natural clay-rock, the Opalinus clay in Switzerland. Swelling pressures were measured by *Madsen and Vonmoos* [1985] for this shale. The clay fraction of this shale is made of kaolinite, illite, mixed layers of illite/smectite (I/S) and small amounts of chlorite [*Bradbury and Baeyens*, 1998]. The swelling behavior of the material is attributed to the presence of the I/S and more precisely to their smectitic content. A 30% fraction of swelling smectite in the I/S which represents almost 17% in weight of the shale was determined by *Madsen and Vonmoos* [1985]. The other fractions for the remaining clay minerals were not provided by these authors. But, considering the high value of the total specific surface

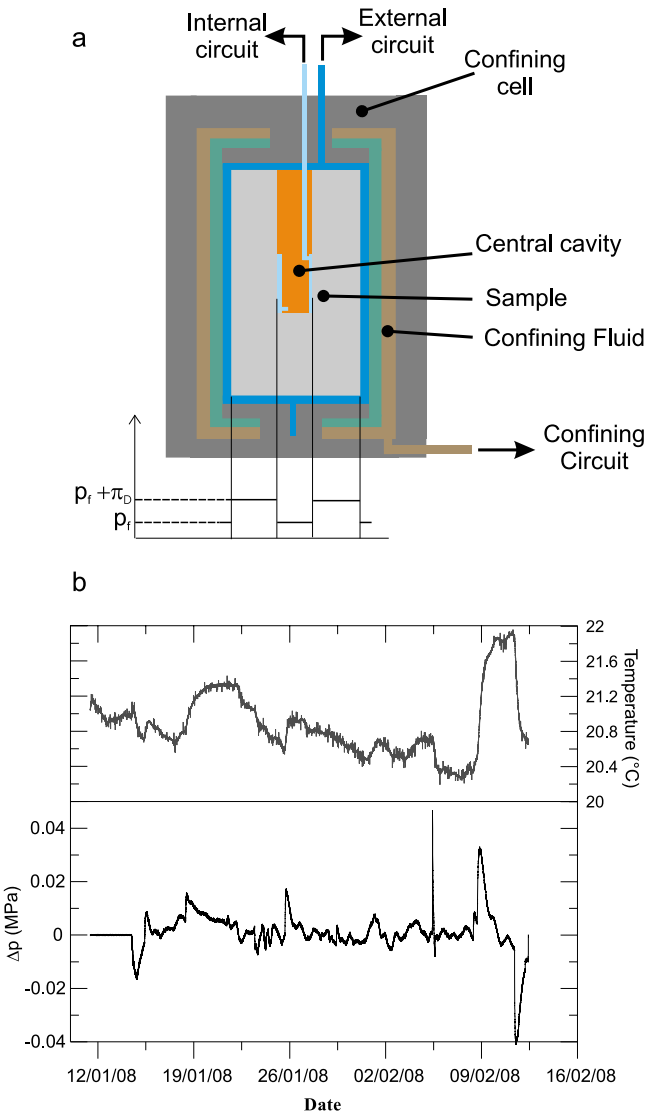

Figure 6. (a) Experimental design for sample-scale osmotic experiments [*Rousseau-Gueutin et al.*, 2009]. A cylindrical sample where a central hole is drilled is placed in a triaxial press. The external and the internal circuits allow us to impose a concentration gradient. (b) Pressure difference Δp between the internal and external circuits in the absence of a salinity gradient. The variations around zero are only due to room temperature changes.

of smectite (see Figure 3c, internal plus external surfaces, 750 $m^2\ g^{-1}$) in comparison with illite (70 $m^2\ g^{-1}$) or kaolinite (15 $m^2\ g^{-1}$), a dominant smectite surface fraction f_S^{sm} is expected. Indeed, the fraction of the total specific surface of the shale corresponding to smectite $f_{wt}^{sm} A_S^{sm}$ is 38 $m^2\ g^{-1}$ (30% of the 17% weight fraction of I/S, with A_S^{sm} = 750 $m^2\ g^{-1}$) while the average total specific surface area (including internal surfaces) of the shale $\sum_k f_{wt}^k A_S^k$ was estimated to be 70 $m^2\ g^{-1}$ by these authors. According to equation (19), this yields a surface fraction for the smectite, f_S^{sm}, of 54%. In addition, the disjoining pressure for smectite is up to 1 order of magnitude higher than for illite particles and the values for kaolinite can be neglected. Consequently, only the contribution of smectite was considered in equation (20). The equilibrium concentration was estimated to be 10^{-2} mol L^{-1} by *Madsen and Vonmoos* [1985]. In their study, *Madsen and Vonmoos* [1985] used an expression similar to equation (21) with the total specific surface to identify the interparticle spacings. This provides an estimate of the average interparticle space including the nonmobile water in the interlayers of the smectite minerals involved in the swelling. An alternative approach is to consider only the external specific area to identify a mean pore size. This corresponds in fact to the "hydrodynamic" pore size, i.e., the pores between aggregates where fluid flow can occur. Figure 5 shows the result of the application of the simple averaging approach presented here using equation (20), the disjoining pressure data for the smectite taken from Figure 4 and a value of 0.54 for f_S^{sm}. A good agreement is obtained between the swelling pressure data of *Madsen and Vonmoos* [1985] and this calculation.

4. Impact on the Hydrogeology Study of a Clay-Rich System

[19] For clay materials, the existence of surface forces results in an alteration of the "pressure" in the porosity of a clay. Consequently, this "pressure" should be higher than the hydrostatic pressure in surrounding aquifers at equilibrium with the clay in the case of diffuse layer overlapping. The concepts and calculations developed in sections 2 and 3 lead to the following question: May the current view of hydrogeologists on such media be altered? In order to answer this question, the real significance of such a pressure and its implications for hydrogeology is analyzed below. In an OECD report [*Horseman et al.*, 1996], these authors, describing this concept as a "provoking idea," suggest that the higher permanent pressure in the clay should be interpreted in terms of a threshold (an entry pressure value) for Darcy's law. This idea is also discussed below.

4.1. Implications for Fluid Flow

[20] As proposed by *Derjaguin et al.* [1987], and formalized by different authors [e.g., *Sherwood*, 1994; *Moyne and Murad*, 2002; *Revil and Leroy*, 2004], fluid flow across a clay-rock is proportional to the gradient of the "hydrodynamic" or "partial" pressure $p_f = p_N - \pi_D$, i.e., the bulk or equilibrium solution pressure. This suggests that the disjoining pressure has no direct impact on fluid flow. This idea is supported by experimental work on core samples in contact with reservoirs. Indeed, such disjoining pressures are measured in clay samples at mechanical and thermodynamic equilibrium corresponding to no-flow conditions (no fluid expelled from or attracted toward the pore space). Hence, the existence of this disjoining pressure which constitutes an "excess pressure" relative to the pressure in the reservoirs in the experiments by *Viani et al.* [1983], is not associated with any fluid flow toward the reservoir at equilibrium. This was also verified during our own osmotic experiments at the sample scale in a geometry shown in Figure 6a [*Rousseau-Gueutin et al.*, 2009]. When the same salinity is imposed on the external surface and in a chamber located in a central well within a cylindrical core sample, the same equilibrium pressure p_f is observed in the two reservoirs (see Figure 6b, Δp = 0). Therefore, this higher pressure in the clay-rock

cannot be interpreted as an "overpressure" (pressures exceeding the hydrostatic value, see review by *Neuzil* [1995]) generating diverging flow toward adjacent aquifers. Such erroneous interpretations can be avoided simply by considering the partial or hydrodynamic pressure gradient. This hydrodynamic or partial pressure corresponds to the pressure of water within the reservoirs at the ends of a core sample, for instance. Only in the case of a perturbation of the thermodynamic equilibrium, i.e., a gradient in hydrodynamic pressure or concentration between the reservoirs, can a flux occur and cause the propagation of a pressure perturbation [*Derjaguin et al.*, 1987]. The thermodynamic equilibrium refers here to the conditions where no pressure or concentration gradients are applied at a constant natural lithostatic load. Note that the reference to this hypothetic initial thermodynamic equilibrium is secondary since constitutive transport equations in deforming porous media can be derived on the basis of nonequilibrium thermodynamics [see, e.g., *Revil*, 2007]. These fluxes are calculated with the well-known coupled flow expressions using pressure and concentration gradients [see, e.g., *Neuzil*, 2000; *Gonçalvès et al.*, 2004; *Revil and Linde*, 2006; *Garavito et al.*, 2006; *Gueutin et al.*, 2007]. The electrical properties of clay surfaces explain the presence of additional driving forces for fluid flow besides the pressure gradient and the gravity, namely the chemical potential gradient of the salt $\nabla\mu_f$ and the electrical potential gradient $\nabla\psi$. These other forces are taken into account in a recent model based on the Nernst-Planck and the Navier-Stokes equations and developed by *Revil et al.* [2005]. Introducing the condition that no macroscopic current density occurs in natural materials and after some algebraic manipulations, these authors derive the following equation for the coupled flow system, i.e., a generalized Darcy's law (neglecting gravity effects, i.e., in an almost horizontal flow problem) and a mass transport equation

$$q = -\frac{k}{\mu_f}\nabla p_f + \frac{\alpha_f R_g T \varepsilon k}{\mu_f}\nabla c_f \tag{22}$$

$$\phi_c = (1-\varepsilon) q c_f - D^{eff}\nabla c_f, \tag{23}$$

where q is the specific discharge (m s^{-1}), ϕ_c is the solute flux (mol m^{-2} s^{-1}), α_f is the number of dissociated ions (2 for NaCl salt), c_f (mol L^{-1}) the concentration of the reservoirs at local equilibrium with the shale, k is the intrinsic permeability and ε is the so-called osmotic efficiency whose expression, not developed here [see *Revil et al.*, 2005], involves electrical terms, and D^{eff} is the effective diffusion coefficient (m^2 s^{-1}) also depending on electrical terms. Note that, more rigorously, vectors and tensors should be used in equations (22) and (23) for the fluxes and the coupling coefficients, respectively. A dispersivity tensor should also be used in equation (23). Expressions (22) and (23) illustrate, as discussed by, e.g., *Moyne and Murad* [2002] and *Revil et al.* [2005], that the fluid flow depends on the gradients of p_f and c_f, respectively, the pressure and salinity that would be measured in a reservoir at local equilibrium with the clay-rock. The full resolution of a coupled-flow problem requires the simultaneous calculation of the salt transport and fluid flow that involves the same driving forces.

[21] Another consequence of this concept of disjoining pressure is its possible interpretation as a pressure threshold to generate water filtration through argillaceous media [*Horseman et al.*, 1996]. Although attractive, this interpretation should be used with caution in the light of the above analysis, this pressure is considered inefficient for fluid flow as it is associated with a local stress balance. The controversial idea of the existence of a pressure gradient threshold for fluid flow in clay-rocks has been supported by filtration experiments at the sample scale. Some authors found that below a certain pressure gradient value, no filtration is observed (see discussion by *Mitchell* [1993]). Among the different explanations proposed by *Mitchell* [1993] for these observations, a non-Newtonian behavior or experimental errors can be cited. A Bingham fluid behavior characterized by the presence of a shear stress yield in the relationship between shear stress and the derivative of the fluid velocity could be invoked. But there is no clear evidence of such behavior for the solutions within the porosity of a clay. The experimental errors are discussed below in the light of the coupled equations for fluid flow and transport, i.e. equations (22) and (23). Indeed, the plausibility of a potential threshold effect has to be identified through an analysis of other forces than pressure gradients involved in water movement in such media. If one considers a fluid flow problem under constant salt concentrations ($\nabla c_f = 0$), expression (22) does not introduce any threshold, i.e., as $\nabla p = 0$, $q = 0$. Conversely in the presence of a concentration gradient across a sample, we can obtain q = 0 for nonzero values of ∇p. Possible experimental errors can thus lead to erroneous interpretations of the filtration velocity. For instance, if the zero concentration gradient across the sample is not guaranteed during the experiment, the interpretation in terms of a classical Darcy law (only ∇p) does not capture the real filtration rate (i.e., including the driving force ∇c_f, see equation (22)). These considerations are in line with the discussion by *Mitchell* [1993] who also states that careful experiments on clay materials did not show such yield behavior.

4.2. Implications for the Storativity

[22] If the direct influence of π_D is zero for fluid flow, its implications for effective stress calculations should be more relevant as pointed out by *Horseman et al.* [1996]. As inferred from a local stress balance, the total "pressure" which is effectively acting on the solid surface must be introduced in the effective stress expression $\boldsymbol{\sigma}^{eff}$ that writes classically

$$\boldsymbol{\sigma}^{eff} = \boldsymbol{\sigma} - b_B p_f \mathbf{I}, \tag{24}$$

where $\boldsymbol{\sigma}$ is the total stress, $\mathbf{I}$ is the unit tensor and b_B is the Biot coefficient. This effective stress is involved in the hydromechanical coupling (through the right-hand side of equation (25); see Appendix B) that introduces a fundamental parameter, the specific storage coefficient S_s, in the so-called hydrogeological diffusivity or pressure diffusion equation [see, e.g., *de Marsily*, 1986]:

$$\nabla(\rho_f q) = -\frac{\partial(\rho_f \omega)}{\partial t}. \tag{25}$$

In this section, our goal is to develop a simple hydro-chemomechanical term to be added in the pressure diffusion

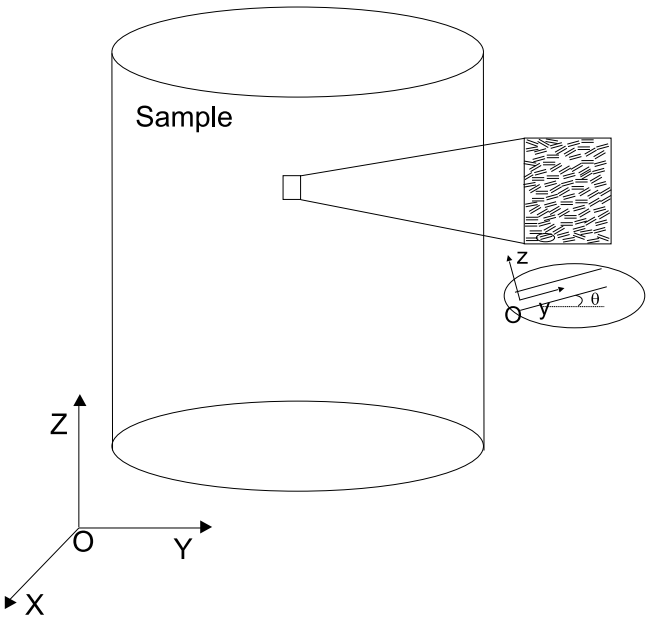

Figure 7. Schematic representation of the averaging approach.

equation (25) in order to account for the swelling of clay-rocks. The introduction of the swelling was considered in soil sciences by, e.g., *Barbour and Fredlund* [1989] or *Hueckel* [1992] or in rock mechanics by, e.g., *Sherwood* [1992, 1994], *Dormieux et al.* [2003], *Gajo et al.* [2002], or *Loret et al.* [2002]. Although the developments proposed by the rock mechanists are rigorous, their practical use for hydrogeologic applications is puzzling. In addition, these developments do not always account for the different components of the disjoining pressure underlying the swelling pressure. The "osmotic" term, i.e., the electrostatic component, is often considered alone. Here we adopt the pragmatic approach discussed by *Neuzil* [2003], i.e., a development with physical basis but using some simplifications which allow a practical introduction of the swelling pressure in hydrogeological studies.

[23] We should now introduce the "total pressure" acting on the solid skeleton of the clay-rich porous medium into the development proposed by *de Marsily* [1986] for the right-hand side of equation (25). For practical use, we need to establish a macroscopic pressure based on the microscopic view presented in section 2.2 which is valid at the pore scale. This is done using a simple rotation (around the x axis) accounting for the mean orientation of the clay particles as depicted in Figure 7 and by taking average values denoted by the angle brackets for the components of **p**. One can determine the average expression of this tensor over the REV in the OXYZ fixed referential:

$$\langle \mathbf{p}_{OXYZ} \rangle = \begin{vmatrix} \langle p_T \rangle & 0 & 0 \\ 0 & \langle p_T \cos^2\theta + p_N \sin^2\theta \rangle & \langle (p_N - p_T)\sin\theta\cos\theta \rangle \\ 0 & \langle (p_N - p_T)\sin\theta\cos\theta \rangle & \langle p_T \sin^2\theta + p_N \cos^2\theta \rangle \end{vmatrix}, \tag{26}$$

where θ is the angle between a clay particle and the y axis (see Figure 7). In order to simplify the notation, we omit the angle brackets and the subscript OXYZ and denote the macroscopic (anisotropic) "pressure" $\boldsymbol{p}$. Considering the notion of effective stress introduced by Terzaghi and extending this notion to the electrochemical processes [*Barbour and Fredlund*, 1989], one obtains

$$\boldsymbol{\sigma}^{\boldsymbol{eff}} = \boldsymbol{\sigma} - b_B \boldsymbol{p}. \tag{27}$$

For small 3D deformations and in the framework of elasticity (noting compression as positive) [*Coussy*, 2004],

$$\frac{dV}{V} \simeq tr(\varepsilon) = -\frac{1-2\nu}{E_Y} tr\left(d\boldsymbol{\sigma}^{\boldsymbol{eff}}\right), \tag{28}$$

where V is the volume of porous medium, ε is the strain tensor, tr is the trace operator, ν and E_Y are the nondimensional Poisson ratio and the Young modulus (Pa). This yields

$$\frac{dV}{V} = -\alpha(tr(d\boldsymbol{\sigma})/3 - b_B/3 tr(d\mathbf{p})), \tag{29}$$

where

$$\alpha = \frac{3(1-2\nu)}{E_Y} \tag{30}$$

is the compressibility of the porous medium (Pa^{-1}) under drained conditions. In order to obtain a first-order expression for practical use, a simplifying assumption for p_T is used. The term $\frac{1}{\epsilon}\frac{\partial \epsilon}{\partial \rho_f}\rho_f$ appearing in equation (15) for p_T can be expressed as $\frac{1}{\epsilon}\frac{\partial \epsilon}{\partial p}\frac{1}{\beta_l}$ using the state equation for water in isothermal conditions where β_l (Pa^{-1}) is the water compressibility. According to the experimental work by *Owen et al.* [1961] or *Anderson et al.* [2000] on the dependence of the dielectric constant of water on the pressure, the term $\frac{1}{\epsilon}\frac{\partial \epsilon}{\partial \rho_f}\rho_f$ is close to one ($\frac{1}{\epsilon}\frac{\partial \epsilon}{\partial p} = 4.71\ 10^{-10}$ Pa^{-1} and $\beta_l = 4.52\ 10^{-10}$ Pa^{-1} at 25°C). For the sake of simplicity, we will thus consider that $p_T = p_f + \pi_D$. Note that by making this assumption, the anisotropy of the "pressure" tensor is neglected since $\mathbf{p} = (p_f + \Pi_D)\mathbf{I}$, with $\Pi_D = \langle \pi_D \rangle$, the macroscopic swelling pressure. We consider also that the clay particles are aligned almost perpendicularly to the lithostatic charge, i.e., are horizontal. Under these assumptions, equation (29) becomes

$$\frac{dV}{V} = -\alpha\left(tr(d\boldsymbol{\sigma})/3 - b_B dp_f - b_B d\Pi_D\right). \tag{31}$$

The first two terms on the right-hand side of equation (31) are the only terms taken into account in the analysis by *de Marsily* [1986] to derive the specific storage coefficient, the last term accounts for the chemomechanical coupling. In order to account for this chemomechanical effect, the last term on the right-hand side of equation (31) can be introduced into the development proposed by Marsily. In the framework of small deformations, i.e., weak variations of the porosity, b_B is constant but dependent on ω [see, e.g., *Cosenza et al.* [2002] and the mass balance equation now writes (see developments in Appendix B)

$$div\left(\rho_f q\right) = -\frac{S_S}{g}\frac{\partial p_f}{\partial t} - S_S^c \frac{\partial c_f}{\partial t}, \tag{32}$$

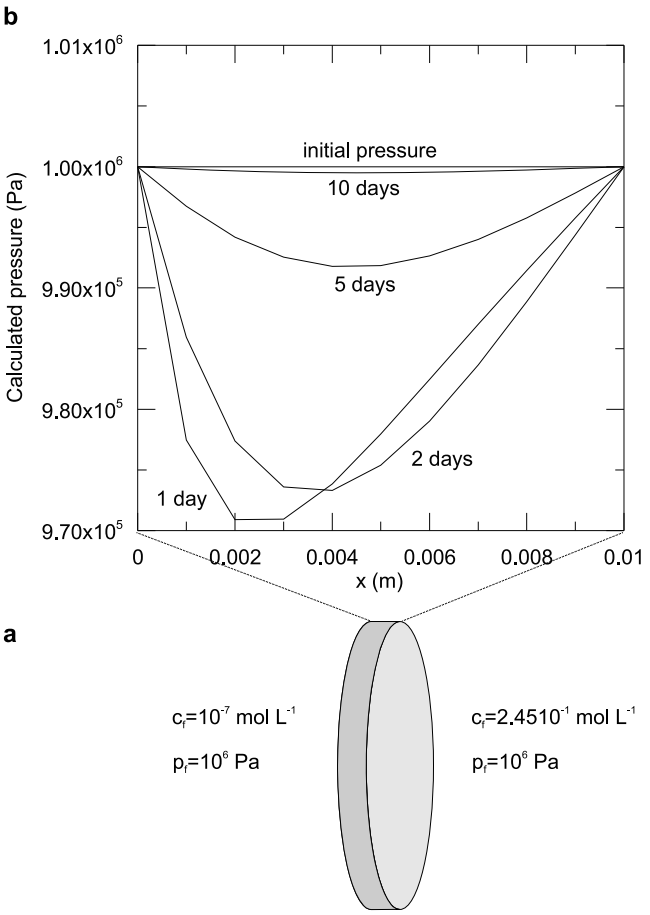

Figure 8. (a) Geometrical setting of the swelling experiment and (b) calculated pressure profiles as functions of time. Parameters used in the calculations are from *Horseman et al.* [2007]: $\omega = 0.15$, $k = 7.9 \times 10^{-21}$ m^2, $S_S = 4.1 \times 10^{-4}$ m^{-1}, $D^{eff} = 1.5 \times 10^{-11}$ m^2 s^{-1}, and $\varepsilon_c = 0.04$.

where S_S (m^{-1}) is the well-known specific storage coefficient and

$$S_S^c = \frac{S_S}{g}\frac{\partial \Pi_D}{\partial c_f} \tag{33}$$

is an "electrochemical specific storage coefficient." For small deformations, the swelling pressure only depends on the salinity c_f and this dependence can be determined by the analysis presented in section 2.3 with the petrophysical characteristics of the shale. Once determined, this relation between the swelling pressure and the salinity can be used to calculate the effect of a salinity perturbation in a shale formation.

[24] The development presented here was applied to a real case study, i.e., the Opalinus clay at Mont Terri, Switzerland [*Horseman et al.*, 2007]. A core sample (a 1 cm thick disc of 5 cm radius) of this material is at equilibrium when both sides of the sample are in contact with a solution corresponding to the formation equilibrium concentration, 0.245 mol L^{-1}. A maximum 0.8% swelling ($\Delta V/V$) was observed by *Horseman et al.* [2007] when one side of this sample was suddenly placed in contact with distilled water. This can be readily understood in the light of the analysis presented in section 3. When a sample is exposed to a solution of lower salinity than its equilibrium solution, the swelling pressure and thus the effective force acting on the solid surfaces increases whence the possible swelling of the material. This experiment is schematically represented in Figure 8a. The transient hydrochemomechanical behavior of this sample was calculated using a 1D finite difference scheme. Equation (22) was combined with equation (32) and the transport expression (23) was combined with the mass conservation equation

$$div(\omega c_f) = \frac{\partial(\omega c_f)}{\partial t} \tag{34}$$

to solve the coupled flow problem. The parameter values given by *Horseman et al.* [2007] are listed in the caption of Figure 8. The swelling deformation $\Delta V/V$ was calculated at each time step by summing the individual deformations of each node i dV_i and by using equation (31) where $d\boldsymbol{\sigma} = 0$ (constant total stress). The term $b_B\alpha$ is obtained using the theoretical expression of S_S, and neglecting the compressibility of water and solids. In the model, the distilled water was represented by a 10^{-7} mol L^{-1} solution. An expression for the swelling pressure as a function of the salinity is required. It was assumed again that the swelling is mostly due to smectite so that only the disjoining pressure for this mineral is considered in equations (19) and (20). In the absence of a precise mineralogical definition of the sample studied by these authors, the average weight fractions for the different clay minerals given by *Nagra* [2002] for the Opalinus clay at the same location were considered, i.e., 14 ± 4% I/S, 18 ± 6% illite, 17 ± 6% kaolinite and 5 ± 2% chlorite. The specific surfaces introduced in equation (19) are 750, 70, 15 and 70 m^2 g^{-1} for smectite, illite, kaolinite and chlorite, respectively. An average value of the total specific surface of 70 m^2 g^{-1} with a porosity of 15% gives a 1 nm value for the average pore size accounting for the interlayers of the smectite fraction in the I/S. Using this estimate of the interparticle distance and the data shown in Figure 4, a relation of the type $\pi_D^0 c_f^n$ for the disjoining pressure of smectite was identified with $\pi_D^0 = 1.59\ 10^6$ Pa and $n = 0.164$. This expression multiplied by the surface fraction of smectite f_S^{sm} (neglecting the other clay minerals contributions) provides the required relation between the swelling pressure and the concentration c_f for the numerical treatment. This fraction of smectite f_S^{sm} was calculated using equation (19), the average weight fraction of I/S (14%) and a proportion of smectite in I/S of 30% [*Madsen and Vonmoos*, 1985]. Figure 8b shows the calculated effect of the swelling of the shale, i.e., a decrease of the pressure. The initial pressure profile is then recovered in 10 days due to the constant pressure boundary conditions applied to the system. The calculated swelling is presented in Figure 9. The use of the average mineralogical composition given above yields a reasonable agreement with the data although a small underestimation can be noted. This discrepancy can be attributed to the simplifying assumptions used to introduce the swelling in the hydrogeological formalism.

5. Conclusions

[25] According to the theoretical developments proposed by interface scientists, for highly compacted clay-rocks, i.e.,

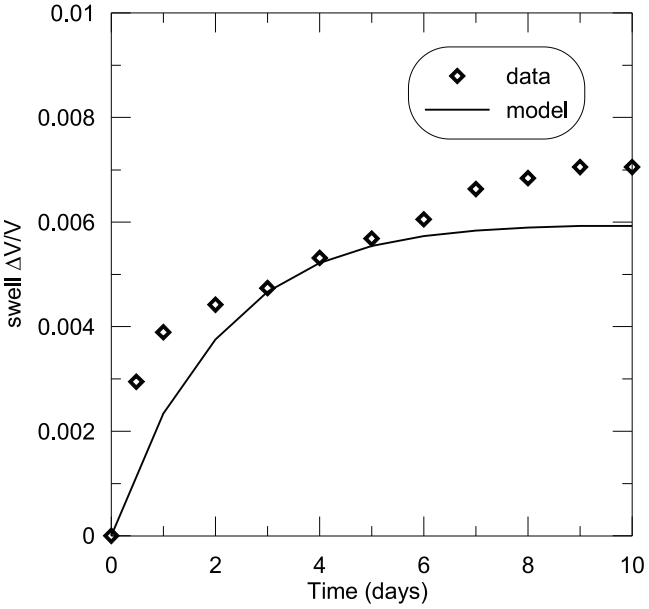

Figure 9. Calculated swelling of the Opalinus shale and data by *Horseman et al.* [2007].

at low porosity, the overlapping of the diffuse layers causes an alteration of the pressure due to the presence of surface forces. The "pressure" is no longer a scalar quantity but becomes a tensor whose components differ from the pressure in the bulk or equilibrium solution. In the case of nonoverlapping diffuse layers (high salinity or large pore sizes), the local pressure in the porosity is not altered and is similar to that of the equilibrium solution. Based on previous theoretical developments, it has been argued here that only the pressure in the equilibrium solution, also called the "hydrodynamic" pressure, is directly involved in fluid flow while the disjoining pressure is associated with a deformation of the porous media. The disjoining pressure is a microscopic concept valid at the pore scale. Although the idea of an "anisotropic pressure" can be confusing or even provoking for fluid mechanists, this could be viewed as a conceptual option followed by *Derjaguin et al.* [1987]. Other scientists, more carefully, consider only surface interaction potential (related to forces upon derivation) or directly surface forces without any further interpretation in terms of fluid pressure. These forces between adjacent surfaces are then used to describe the deformation of the porous skeleton. Whatever the conceptual view, some macroscopic deformations (swelling or shrinking) of charged porous media caused by the alteration of these surface forces are observed. These deformations involve the counterpart of the disjoining pressure at the macroscale (REV), i.e., the swelling pressure, which represents in fact its macroscopic average value. The identification of the swelling pressure for a natural clay-rock requires an upscaling, e.g., a volume averaging approach. In the present paper, a simple method to obtain a macroscopic swelling pressure as a function of the average interparticle spacing and of the concentration of the equilibrium solution in a shale is presented. The main problem arising from this analysis is the determination of a representative interparticle spacing essentially in the smectite fraction which is the main expansive clay mineral. In order to facilitate the introduction of the chemomechanical deformations in the hydrogeological analysis, the available microscopic-scale disjoining pressure data for various clay minerals (some data were presented here) could be collected to create a database. This database could then be used, upon suitable upscalling approaches, to determine the swelling pressure as a function of the pore size and the concentration to be used in a hydrochemomechanical coupling. A first step in this direction was proposed here.

[26] We first answer the question raised at the beginning of section 4 concerning the influence of this disjoining pressure on the hydrogeology in shales. From a mathematical point of view, the main alteration appears in the storativity term of the diffusivity equation with the introduction of an electrochemical storage associated with the swelling of clays. The electrochemical storativity term, which can be mathematically established, depends on the solute transport. Thus, it involves large time scale effects as the transport, dominated by diffusion in such media, is very slow. In addition, the discussion presented here raises the question of our ability to measure the in situ pore pressure and that of the significance of existing pressure measurements. Theoretically, one can design a small measurement chamber imbedded in a shale that would be what [*Coussy*, 2004] calls a "thermodynamic thermometer" (Figure 6a). After some time of local thermodynamic equilibration with the pore space, the water pressure in the chamber is measured. Such measurements are performed in existing devices. According to the theoretical developments presented here, this pressure should be the equilibrium pressure p_f and not the disjoining pressure. However, some influence of the swelling pressure on the pressure measured in the isolated chambers might occur. As discussed in section 3.3, the equilibrium solution in the medium is difficult to predict or measure. When the measurement chambers are initially filled with a solution that is considered to be the equilibrium one, a certain discrepancy with the real solution may exist. This discrepancy can create a swelling of the clay-rock causing a partial closure of the chamber and a subsequent transient increase of the pressure due to the low compressibility of the chamber (fluid, tubing, packers). This transient effect can be detected and should be properly interpreted introducing the swelling pressure but must disappear when chemical equilibrium is reached, after a long time. These concepts are particularly relevant in the present context of scientific research on argillaceous media studied for their potential confining properties of radionuclides.

Appendix A: Electrostatic Component of the Disjoining Pressure

[27] According to *Derjaguin et al.* [1987], the mechanical volumetric force balance equation within a film of water between two charged surfaces imbedded in a bulk (equilibrium) solution writes

$$grad(p) + \rho grad(\varphi) + grad\left(\frac{1}{2}\frac{\partial \epsilon}{\partial \rho_f}\rho_f E^2\right) = 0, \qquad \text{(A1)}$$

with $p(z, b)$ (Pa), the hydrostatic pressure, z the axis perpendicular to the solid surface, ρ the charge density (C m^{-3}) in the film of solution [see also *Van Olphen*, 1963], ρ_f the

density of the fluid (kg m^{-3}) and E the electric field (V m^{-1}). Equation (A1) can be written in a differential form:

$$dp + \rho d\varphi + d\left(\frac{1}{2}\frac{d\epsilon}{d\rho_f}\rho_f E^2\right) = 0. \tag{A2}$$

Equation (A2) can be integrated from the conditions E = 0, $\varphi = 0$, and $p = p_f$ prevailing in the bulk or equilibrium solution and the interplatelet conditions where $E \neq 0$, $\varphi \neq 0$, and $p \neq p_f$ yielding

$$p_f = p(z,b) + \int_0^{\varphi} \rho d\varphi + \frac{1}{2}E^2\frac{\partial\epsilon}{\partial\rho_f}\rho_f. \tag{A3}$$

Equation (A1) written in the z direction, perpendicular to the mineral surface, and corresponding to the direction of the electric field ($E_z \neq 0$, $E_x = E_y = 0$) yields

$$\frac{\partial p(z,b)}{\partial z} + \rho\frac{\partial\varphi(z,b)}{\partial z} + \frac{\partial}{\partial z}\left(\frac{1}{2}\frac{\partial\epsilon}{\partial\rho_f}\rho_f E^2(z,b)\right) = 0. \tag{A4}$$

Noting that

$$-\frac{\partial}{\partial z}\left(\frac{\epsilon E^2}{2}\right) = \rho\frac{\partial\varphi}{\partial z}, \tag{A5}$$

which follows from the definition of the electric field

$$E(z,b) = -\frac{\partial\varphi}{\partial z}, \tag{A6}$$

and the Poisson equation (with a constant value of ϵ)

$$\frac{\partial^2\varphi}{\partial z^2} = -\frac{\rho}{\epsilon}. \tag{A7}$$

Equation (A4) can be written in the form

$$\frac{\partial}{\partial z}\left[p(z,b) - \frac{\epsilon}{2}E^2(z,b) + \frac{1}{2}\frac{\partial\epsilon}{\partial\rho_f}\rho_f E^2(z,b)\right] = 0. \tag{A8}$$

From the last expression, the total pressure normal to the surface in the fluid film can be introduced in the form

$$p_{zz} = p(z,b) - \frac{\epsilon}{2}E^2(z,b) + \frac{1}{2}\frac{\partial\epsilon}{\partial\rho_f}\rho_f E^2(z,b). \tag{A9}$$

From equation (A8), it can be seen that this pressure is independent of z, it depends only on the interplatelet distance $2b$. Introducing the expression for $p(z, b)$ from equation (A3) into equation (A9),

$$p_{zz} - p_f = \pi_D^e = -\int_0^{\varphi}\rho d\varphi - \frac{\epsilon}{2}E^2, \tag{A10}$$

where π_D^e is the electrostatic component of the disjoining pressure. As noted by *Derjaguin et al.* [1987], this component is independent of z and depends only on the interplatelet distance. It can thus be written at the midplane in the special case of identically charged surfaces. At $z = b$, E = 0, $\varphi = \varphi_b$ and thus,

$$\pi_D^e = -\int_0^{\varphi_b}\rho d\varphi. \tag{A11}$$

Introducing the classical Boltzmann distribution corresponding to ideal solutions for a symmetric and monovalent salt, one finds the classical result

$$\pi_D^e = 2k_BTc_f\left(\cosh\left(\frac{e\varphi_b}{k_BT}\right) - 1\right)$$

$$= k_BT\left(c^+ + c^- - 2c_f\right)_{z=b}. \tag{A12}$$

If equation (A1) is expressed in the direction tangential to the surface (x or y), the electric field components being null, the following expression is found:

$$p_{xx} = p_{yy} = p(z,b) = p_f - \int_0^{\varphi}\rho d\varphi - \frac{E^2}{2}\frac{\partial\epsilon}{\partial\rho_f}\rho_f. \tag{A13}$$

The transversal component is thus dependent on the distance to the surface. This illustrates the tensorial property of the total "pressure" introduced by *Derjaguin et al.* [1987]. A more convenient expression for these components can be found by introducing the electrostatic component of the disjoining pressure. For this purpose, equation (A5) written in a differential form is integrated from the conditions E = 0, $\varphi = \varphi_b$ and the condition where the electric field and the electrical potential are E and φ. This yields

$$\int_0^{\varphi}\rho d\varphi = \int_0^{\varphi_b}\rho d\varphi - \frac{\epsilon}{2}E^2. \tag{A14}$$

Introducing equation (A14) into equation (A13), using equation (A11) and renaming this component p_T yields

$$p_T = p_f + \frac{1}{\epsilon}\frac{\partial\epsilon}{\partial\rho_f}\rho_f\pi_D^e + \left(\frac{1}{\epsilon}\frac{\partial\epsilon}{\partial\rho_f}\rho_f - 1\right)\int_0^{\varphi}\rho d\varphi. \tag{A15}$$

Similarly, renaming the component of the pressure normal to the surface p_N, the latter writes

$$p_N = p_f + \pi_D^e. \tag{A16}$$

Appendix B: Development of a Storage Coefficient Accounting for the Chemical Couplings

[28] Noting that Darcy's velocity is in fact a filtration relative to the solid matrix, the continuity equation equation (25) is written by [e.g., *de Marsily*, 1986]

$$-div\left(\rho_f q\right) = \omega\frac{d\rho_f}{dt} + \frac{\rho_f}{1-\omega}\frac{d\omega}{dt} - \frac{\rho_f\omega}{\rho_S}\frac{d\rho_S}{dt}, \tag{B1}$$

where ρ_f and ρ_S are the densities of the fluid and the solid (kg m^{-3}), respectively; q (m s^{-1}) is the specific discharge and ω is the porosity and d/dt is the material derivative following the mean movement of the solid. Assuming a total pressure $\mathbf{p} = (p_f + \Pi_D)\mathbf{I}$, and introducing Biot's coefficient in the hydromechanical coupling analysis of *de Marsily* [1986] yields

$$\frac{d\rho_f}{dt} = \rho_f\beta_l\frac{d\left(p_f + \Pi_D\right)}{dt}, \tag{B2}$$

$$\frac{d\omega}{dt} = ((1-\omega)\alpha - \omega\beta_S)b_B\frac{d\left(p_f + \Pi_D\right)}{dt}, \tag{B3}$$

$$\frac{d\rho_S}{dt} = \rho_S\frac{\beta_S\omega}{1-\omega}\frac{d\left(p_f + \Pi_D\right)}{dt}. \tag{B4}$$

Introducing equation (B2) to (B4) into equation (B1) yields

$$div(\rho_f q) = -\frac{S_S}{g}\frac{d(p_f + \prod_D)}{dt}, \tag{B5}$$

with

$$S_S = \rho_f g \omega \left[\beta_l - \beta_S + b_B \frac{\alpha}{\omega}\right], \tag{B6}$$

the specific storage coefficient (m^{-1}). For small deformations, it is assumed that the swelling pressure depends only on the salinity c_f and equation (B5) can be written in the desired form

$$div(\rho_f q) = -\frac{S_S}{g}\frac{dp_f}{dt} - S_S^c \frac{dc_f}{dt}, \tag{B7}$$

with

$$S_S^c = \frac{S_S}{g}\frac{d\prod_D}{dc_f}. \tag{B8}$$

S_S^c is an "electrochemical specific storage coefficient." Noting that the velocity of the solid is very small, the material derivatives can be substituted by the ordinary derivatives ($\partial/\partial t$, see equations (32) and (33) in the text).

Notation

A	Hamaker constant, J.
A_S	specific surface, $m^2\ kg^{-1}$.
A_S^i	specific surface of mineral i, $m^2\ kg^{-1}$.
b	half-pore size, m.
b_B	Biot's coefficient.
c_i	concentration of ion i in the porosity, ion m^{-3} or mol L^{-1}.
c_f^i	concentration of ion i in the equilibrium solution, ion m^{-3} or mol L^{-1}.
c_f	concentration of symmetric ions in the equilibrium solution, ion m^{-3} or mol L^{-1}.
D^{eff}	effective diffusion coefficient, $m^2\ s^{-1}$.
E	electric field, V m^{-1}.
E_Y	Young modulus, Pa.
e	elementary charge, C.
f_S^i	surface fraction of mineral i.
f_{wt}^i	weight fraction of mineral i.
k	intrinsic permeability, m^2.
k_B	Boltzmann constant, J K^{-1}.
p_f	pressure in the equilibrium solution, Pa.
p	"pressure" tensor in a film, Pa.
p_N, p_T	normal and transverse components of **p**, Pa.
q	Darcy's velocity, m s^{-1}.
q_i	ionic charge, C.
R_g	Gas constant, m^3 Pa K^{-1} mol^{-1}.
S_S	specific storage coefficient, m^{-1}.
T	temperature, K.
V	volume of porous medium, m^3.
α	compressibility of the porous medium, Pa^{-1}.
β_l	compressibility of the fluid, Pa^{-1}.
β_S	compressibility of the solid grains, Pa^{-1}.
ϵ	permittivity of the fluid, F m^{-1}.
ε_c	osmotic efficiency.
$\boldsymbol{\varepsilon}$	strain tensor.
φ	electrical potential, V.
η_f	dynamic viscosity of the equilibrium solution, Pa s.
ν	Poisson ratio.
ν_i	valency of ion i.
π_D	disjoining pressure, Pa.
π_D^e	electrostatic component of the disjoining pressure, Pa.
π_D^{vdw}	molecular component of the disjoining pressure, Pa.
π_D^s	structural component of the disjoining pressure, Pa.
$\langle \pi_D \rangle$ or $\prod_D$	swelling pressure, Pa.
ρ	charge density of the solution, C m^{-3}.
ρ_f	density of the equilibrium solution, kg m^{-3}.
ρ_S	solid density, kg m^{-3}.
$\boldsymbol{\sigma}$	total stress tensor, Pa.
$\boldsymbol{\sigma}^{eff}$	effective stress tensor, Pa.
ω	porosity.

[29] **Acknowledgments.** The French National Center for Scientific Research (CNRS) through the scientific program ECCO-PEER and the French Nuclear Waste Agency Andra are acknowledged for their support. We also thank three anonymous reviewers for the help in improving a first draft of this paper, as well as the Associate Editor for his clear comments and suggestions.

References

Anderson, G., R. Miller, and A. Goodwin (2000), Static dielectric constants for liquid water from 300 K to 350 K at pressures to 13 MPa using a new radio-frequency resonator, *J. Chem. Eng. Data*, *45*, 549–554.

Barbour, S., and D. Fredlund (1989), Mechanisms of osmotic flow and volume change in clay soils, *Can. Geotech. J.*, *26*, 551–562.

Barclay, L., and R. Ottewill (1970), Measurement of forces between colloidal particles, *Spec. Discuss. Faraday Soc.*, *1*, 138–147.

Bennethum, L., and T. Weinstein (2004), Three pressures in porous media, *Transp. Porous Media*, *54*, 1–34.

Bennethum, L., M. A. Murad, and J. H. Cushman (1997), Modified Darcy's law, Terzaghi's effective stress principle and Fick's law for swelling clay soils, *Comput. Geotech.*, *20*, 245–266.

Bradbury, M., and B. Baeyens (1998), A physicochemical characterisation and geochemical modelling approach for determining porewater chemistries in argillaceous rocks, *Geochim. Cosmochim. Acta*, *62*, 783–795.

Callaghan, I., and R. Ottewill (1974), Interparticle forces in montmorillonite gels, *Discuss. Faraday Soc.*, *57*, 110–118.

Churaev, N. (2003), Derjaguin's disjoining pressure in the colloid science and surface phenomena, *Adv. Colloid Interface Sci.*, *104*, xv–xx.

Cosenza, P., M. Ghoreychi, G. de Marsily, G. Vasseur, and S. Violette (2002), Theoretical prediction of poroelastic properties of argillaceous rocks from in situ specific storage coefficient, *Water Resour. Res.*, *38*(10), 1207, doi:10.1029/2001WR001201.

Coussy, O. (2004), *Poromechanics*, John Wiley, Chichester, U. K.

Davis, J., and J. Leckie (1978), Surface ionization and complexation at the oxide/water interface. 2. Surface properties of amorpheous iron oxyhydroxide and adsorption of metal ions, *J. Colloid Interface Sci.*, *67*, 90–107.

de Marsily, G. (1986), *Quantitative Hydrogeology, Groundwater Hydrology for Engineers*, Academic, New York.

de Marsily, G., J. Gonçalvès, S. Violette, and M. Castro (2002), Migration mechanisms of radionuclides from a clay repository toward adjacent aquifers and the surface, *C. R. Acad. Sci. Phys.*, *3*, 945–959.

Derjaguin, B. V., N. V. Churaev, and V. M. Muller (1987), *Surface Forces*, 1st ed., Consult. Bur., New York.

Dormieux, L., E. Lemarchand, and O. Coussy (2003), Macroscopic and micromechanical approaches to the modelling of the osmotic swelling in clays, *Transp. Porous Media*, *50*, 75–91.

Gajo, A., B. Loret, and T. Hueckel (2002), Electro-chemo-mechanical couplings in saturated porous media: Elastic-plastic behaviour of heteroionic expansive clays, *Int. J. Solids Struct.*, *39*, 4327–4362.

Garavito, A., H. Kooi, and C. Neuzil (2006), Numerical modeling of a long-term in situ chemical osmosis experiment in the Pierre Shale, South Dakota, *Adv. Water Resour.*, *29*(3), 481–492.

Gonçalvès, J., and P. Rousseau-Gueutin (2008), Molecular-scale model for the mass density of electrolyte solutions bound by clay surfaces: Application to bentonites, *J. Colloid Interface Sci.*, *320*, 590–598.

Gonçalvès, J., S. Violette, and J. Wendling (2004), Analytical and numerical solutions for alternative overpressuring processes: Application to the Callovo-Oxfordian sedimentary sequence in the Paris basin, France, *J. Geophys. Res.*, *109*, B02110, doi:10.1029/2002JB002278.

Gonçalvès, J., P. Rousseau-Gueutin, and A. Revil (2007), Introducing interacting diffuse layers in TLM calculations. A reappraisal of the influence of the pore size on the swelling pressure and the osmotic efficiency of compacted bentonites, *J. Colloid Interface Sci.*, *316*, 92–99.

Gueutin, P., S. Altmann, J. Gonçalvès, P. Cozensa, and S. Violette (2007), Osmotic interpretation of overpressures from monovalent based triple layer model, in the Callovo-Oxfordian at the Bure site, *Phys. Chem. Earth*, *32*, 434–440.

Heidug, W., and S. -W. Wong (1996), Hydration swelling of water-absorbing rocks: A constitutive model, *Int. J. Numer. Anal. Methods Geomech.*, *20*, 403–430.

Hiemstra, T., and W. H. Van Riemsdijk (1996), A surface structural approach to ion adsorption: The charge distribution (CD) model, *J. Colloid Interface Sci.*, *179*, 488–508.

Horseman, S. T., J. J. W. Higgo, J. Alexander, and J. F. Harrington (1996), *Water, Gas and Solute Movement Trough Argillaceous Media*, Nucl. Energy Agency, Issy-les-Moulineaux, France.

Horseman, S., J. F. Harrington, and D. J. Noy (2007), Swelling and osmotic flow in a potential host rock, *Phys. Chem. Earth*, *32*, 408–420.

Hribar, B., N. Southall, V. Vlachy, and K. A. Dill (2002), How ions affect the structure of water, *J. Am. Chem. Soc.*, *124*, 12,302–12,311.

Huang, S., N. Aughenbaugh, and J. Rockaway (1986), Swelling pressure studies of shales, *Int. J. Rock Mech. Min. Sci.*, *23*, 371–377.

Hueckel, T. (1992), On effective stress concepts and deformation in clays subjected to environmental loads: Discussion, *Can. Geotech. J.*, *29*, 1120–1125.

Israelachvili, J. N., and G. Adams (1978), Surface force apparatus, *J. Chem. Soc. Faraday Trans. 1*, *74*, 975–1001.

Israelachvili, J. N., and R. M. Pashley (1983), Molecular layering of water at surfaces and origin of repulsive hydration forces, *Nature*, *306*, 249–250.

Jougnot, D., A. Revil, and P. Leroy (2009), Diffusion of ionic tracers in the callovo-oxfordian clay-rock using the Donnan equilibrium model and the electrical formation factor, *Geochim. Cosmochim. Acta*, *73*, 2712–2726.

Langmuir, I. (1938), The role of attractive and repulsive forces in the formation of tactoids, thixotropic gels, protein crystals and coacervates, *J. Chem. Phys.*, *6*, 873–896.

Leroy, P., and A. Revil (2004), A triple-layer of the surface electrochemical properties of clay minerals, *J. Colloid Interface Sci.*, *270*, 371–380.

Li, H., J. Long, Z. Xu, and J. Masliyah (2007), Flocculation of kaolinite clay suspensions using a temperature-sensitive polymer, *Am. Inst. Chem. Eng. J.*, *53*, 479–488.

Loret, B., T. Hueckel, and A. Gajo (2002), Chemo-mechanical coupling in saturated porous media: Elastic-plastic behaviour of homoionic expansive clays, *Int. J. Solids Struct.*, *39*, 2773–2806.

Low, P. (1987), Structural component of the swelling pressure of clays, *Langmuir*, *3*, 18–25.

Madsen, F., and M. Vonmoos (1985), Swelling pressure calculated from mineralogical properties of a Jurassic Opalinum shale, Switzerland, *Clays Clay Miner.*, *33*, 501–509.

Marcelja, S., and N. Radic (1976), Repulsion of interfaces due to bound water, *Chem. Phys. Lett.*, *42*, 129–130.

Marion, D., A. Nur, H. Yin, and D. Han (1992), Compressional velocity and porosity in sand-clay mixtures, *Geophysics*, *57*, 554–563.

Martin, S. (1960), Absorded water on clay: A review, *Clays Clay Miner.*, *9*, 28–70.

McBride, M. B. (1997), A critique of diffuse double layer models applied to colloid and surface chemistry, *Clays Clay Miner.*, *45*, 598–608.

McGuiggan, P., and R. Pashley (1988), Molecular layering in thin aqueous films, *J. Phys. Chem.*, *92*, 1235–1239.

Mitchell, J. K. (1993), *Fundamentals of Soil Behavior*, John Wiley, New York.

Moyne, C., and M. Murad (2002), Electro-chemo-mechanical couplings in swelling clays derived from a micro/macro-homogenization procedure, *Int. J. Solids Struct.*, *39*, 6159–6190.

Murad, M., and J. Cushman (1997), A multiscale theory of swelling porous media: II. Dual porosity models for consolidation of clays incorporating physicochemical effects, *Transp. Porous Media*, *28*, 69–108.

Murad, M., and J. Cushman (2000), Thermomechanical theories for swelling porous media with microstructure, *Int. J. Eng. Sci.*, *38*, 517–564.

Nagra (2002), Project Opalinus Clay: Safety report. Demonstration of disposal feasibility (Entsorgungsnachweis) for spent fuel, vitrified high-level waste and long-lived intermediate-level waste, *Tech. Rep. 02-05*, Wettingen, Switzerland. (Available at http://www.nagra.ch/g3.cms/s_page/83210/s_name/shopproductlist1/s_level/10190)

Neuzil, C. E. (1995), Abnormal pressures as hydrodynamic phenomena, *Am. J. Sci.*, *295*, 742–786.

Neuzil, C. E. (2000), Osmotic generation of 'anomalous' fluid pressures in geological environments, *Nature*, *403*, 182–184.

Neuzil, C. E. (2003), Hydromechanical coupling in geologic processes, *Hydrogeol. J.*, *11*, 41–83.

Owen, B., R. Miller, C. Milner, and L. Cogan (1961), The dielectric constant of water as a function of temperature and pressure, *J. Phys. Chem.*, *65*, 2065–2070.

Pashley, R. (1981), Hydration forces between mica surfaces in aqueous electrolyte solutions, *J. Colloid Interface Sci.*, *80*, 153–162.

Quirk, J. (1986), Soil permeability in relation to sodicity and salinity, *Philos. Trans. R. Soc. London, Ser. A*, *316*, 297–317.

Quirk, J., and R. Pashley (1991), Structural component of the swelling pressure of calcium clays, *Aust. J. Soil Res.*, *29*, 209–214.

Revil, A. (2007), Thermodynamics of transport of ions and water in charged and deformable porous media, *J. Colloid Interface Sci.*, *307*, 254–264.

Revil, A., and P. Leroy (2004), Constitutive equations for ionic transport in porous shales, *J. Geophys. Res.*, *109*, B03208, doi:10.1029/2003JB002755.

Revil, A., and N. Linde (2006), Chemico-electromechanical coupling in microporous media, *J. Colloid Interface Sci.*, *302*, 682–694.

Revil, A., P. Leroy, and K. Titov (2005), Characterization of transport properties of argillaceous sediments: Application to the Callovo-Oxfordian argillite, *J. Geophys. Res.*, *110*, B06202, doi:10.1029/2004JB003442.

Rousseau-Gueutin, P., V. de Greef, J. Gonçalvès, S. Violette, and S. Chanchole (2009), Experimental device for chemical osmosis measurement on natural clay-rock samples maintained at in situ conditions. Implications for formation pressure interpretations, *J. Colloid Interface Sci.*, *337*, 106–116.

Sherwood, J. (1992), Ionic motion in a compacting filtercake, *Philos. Trans. R. Soc. London, Ser. A*, *437*, 607–627.

Sherwood, J. D. (1994), A model for the flow of water and ions into swelling shale, *Langmuir*, *10*, 2480–2486.

Sposito, G., N. Skipper, R. Sutton, S. -H. Park, A. Soper, and J. Greathouse (1999), Surface geochemistry of the clay minerals, *Proc. Natl. Acad. Sci. U. S. A.*, *96*, 3358–3364.

Stratton, J. (1941), *Electromagnetic Theory*, McGraw-Hill, New York.

Van Olphen, H. (1963), *An Introduction to Clay Colloid Chemistry for Clay Technologists, Geologists and Soil Scientists*, Wiley Intersci., New York.

Viani, B., P. Low, and C. Roth (1983), Direct measurement of the relation between interlayer force and interlayer distance in the swelling of montmorillonite, *J. Colloid Interface Sci.*, *96*, 229–244.

Wong, R. (1998), Swelling and softening behaviour of La Biche shale, *Can. Geotech. J.*, *35*, 206–221.

P. Cosenza, HydrASA, FRE 3114, ESIP, Université de Poitiers, CNRS, 40 Av. Recteur Pineau, F-86022 Poitiers, France.

G. de Marsily, J. Gonçalvès, and S. Violette, Sisyphe, UMR 7619, case 105, Université Pierre et Marie Curie, 4 pl. Jussieu, F-75252, Paris CEDEX 05, France. (julio.goncalves@upmc.fr)

P. Rousseau-Gueutin, School of the Environment, Flinders University, GPO Box 2100 Adelaide, SA 5001, Australia.